

Plasmon attenuation and optical conductivity of a two-dimensional electron gas

E.G. Mishchenko,^{1,2} M.Yu. Reizer,³ and L.I. Glazman⁴

¹*Lyman Laboratory, Department of Physics, Harvard University, Cambridge, MA 02138*

²*L.D. Landau Institute for Theoretical Physics, Moscow 117334, Russia*

³*5614 Naïche Rd., Columbus, OH 43213*

⁴*Theoretical Physics Institute, University of Minnesota, Minneapolis, MN 55455*

In a ballistic two-dimensional electron gas, the Landau damping does not lead to plasmon attenuation in a broad interval of wave vectors $q \lesssim k_F$. Similarly, it does not contribute to the optical conductivity $\sigma(\omega, q)$ in a wide domain of its arguments, $E_F > \omega > qv_F$, where E_F , k_F and v_F are, respectively, the Fermi energy, wavevector and velocity of the electrons. We identify processes that result in the plasmon attenuation in the absence of Landau damping. These processes are: the excitation of two electron-hole pairs, phonon-assisted excitation of one pair, and a direct plasmon-phonon conversion. We evaluate the corresponding contributions to the plasmon linewidth and to the optical conductivity.

PACS numbers: 73.23.-b, 72.30.+q, 71.45.Gm, 63.22.+m

I. INTRODUCTION

Because of the long-range nature of the Coulomb interaction, the energy of a plasmon propagating in an electron gas exceeds greatly the energy of an electron-hole excitation at the same wave vector q , provided that q is smaller than the Fermi wave vector k_F . This remains true in any dimensionality, including the case of a two-dimensional electron gas (2DEG), for which the plasmon spectrum is gapless,

$$\omega_q = v_F \sqrt{\frac{\kappa q}{2}}; \quad (1)$$

here v_F is the Fermi velocity, $\kappa = 2me^2/\varepsilon^*$ is the inverse screening radius, m is the effective electron mass, and ε^* is the dielectric constant of the host material. (Hereinafter, we use the units with $\hbar = 1$.) High plasmon velocity, $d\omega_q/dq \gg v_F$, prevents plasmon from decaying into an electron-hole pair and makes the Landau damping exponentially small at low temperatures. Therefore, the leading contribution to the plasmon attenuation of a purely electronic nature comes from the plasmon decay into two electron-hole pairs¹. Two such pairs propagating in opposite directions can carry large energy while having a negligible total momentum.

In 2DEG formed in semiconductor heterostructures, there are additional channels for plasmon attenuation. The energy and momentum conservation conditions can also be satisfied for processes in which a plasmon creates an electron-hole pair and a phonon, rather than two electron-hole pairs. We will call an attenuation due to such processes a *phonon-assisted Landau damping* since it involves a single electron-hole pair. The effectiveness of this process is increased by a large phase space for the emission of phonons in the bulk of a semiconductor.

Yet another possibility of the plasmon attenuation in a heterostructure arises from a conversion of the plasmon into an acoustic phonon via a virtual electron-hole pair. Such a process is feasible due to the absence of

momentum conservation in the direction perpendicular to the 2DEG plane (z -direction). This makes it possible to satisfy energy and in-plane momentum conservation conditions for a process in which a plasmon is converted into a phonon with appropriate value q_z of the momentum along z -axis: $\omega_q = s\sqrt{q^2 + q_z^2}$, where s is the sound velocity. Note that processes involving optical phonons can be safely neglected as they have large energy thresholds (typically 35 – 50 meV).

In the present paper, we analyze the mentioned above inelastic processes leading to plasmon attenuation, and do not consider the effect of impurities, assuming 2DEG sufficiently clean. In Section II the plasmon broadening due to plasmon-phonon conversion is discussed. The conversion is mediated by a virtual electron-hole pair with a rate independent of temperature. In subsequent Sections we discuss scattering processes leading to the creation of real electron-hole pairs in the final state: in Section III the probability for plasmon scattering into a phonon and an electron-hole pair is derived. In Section IV we evaluate the rate of plasmon decay into two electron-hole pairs. In Section V we compare the considered mechanisms with each other.

II. PLASMON-PHONON CONVERSION

The Hamiltonian of the 2DEG interacting with phonons has the form,

$$\hat{H} = - \sum_i \frac{\nabla_i^2}{2m} + \sum_{i>j} \frac{e^2}{\varepsilon^* |\mathbf{x}_i - \mathbf{x}_j|} + \sum_{i\lambda} \int \frac{d^3k}{(2\pi)^3} \frac{\mathcal{M}_\lambda(\mathbf{k})}{\sqrt{2\rho\omega_{\lambda\mathbf{k}}}} (\hat{c}_{\lambda\mathbf{k}} e^{-i\omega_{\lambda\mathbf{k}}t + i\mathbf{k}\cdot\mathbf{x}_i} + \text{c.c.}), \quad (2)$$

where the second quantization representation for phonon variables and coordinate representation for electron variables are used. The second term in Eq. (2) stands for the electron-electron interaction and the last term

describes interaction of two-dimensional electrons with three-dimensional phonons: $\mathcal{M}_\lambda(\mathbf{k})$ is the coupling function for the λ -th phonon branch, $\hat{c}_{\lambda\mathbf{k}}$ are the phonon annihilation operators, \mathbf{k}_\parallel denotes the in-plane component of the phonon wave vector \mathbf{k} , and ρ is the density of the crystal. For simplicity, we assume an isotropic phonon spectrum, $\omega_{\lambda\mathbf{k}} = s_\lambda k$.

The electron-phonon interaction in semiconductor heterostructures is mainly due to the deformation potential (both Si- and GaAs-based structures) and piezoelectric coupling (GaAs structures). The deformation potential^{2,3,4},

$$\mathcal{M}_l^2(\mathbf{k}) = \Xi^2(k_\parallel^2 + k_z^2), \quad (3)$$

couples electrons to the longitudinal (l) acoustic phonons only, Ξ being the deformation potential constant.

Piezoelectric interaction (present in GaAs heterostructures) couples electrons both to longitudinal and transverse (t) phonons^{5,6,7},

$$\mathcal{M}_\lambda^2(\mathbf{k}) = 2(eh_{14})^2 \frac{k_\parallel^2}{k^6} \begin{cases} \frac{9}{4} k_\parallel^2 k_z^2, & \lambda = l, \\ k_z^4 + \frac{1}{8} k_\parallel^4, & \lambda = t. \end{cases} \quad (4)$$

Here we utilized the conventional notation for the coupling constant, h_{14} . In contrast to the deformation potential interaction Eq. (3), piezoelectric coupling does not vanish in the long-wavelength limit $\mathbf{k} \rightarrow 0$.

The plasmon dispersion is determined by the solution of the equation $\varepsilon(\omega, q)/\varepsilon^* = 1 - V_q \chi(\omega, q) = 0$. Here $V_q = 2\pi e^2/(q\varepsilon^*)$ stands for the Fourier transform of the Coulomb interaction. The electron polarization operator in the random phase approximation (RPA) is given by

$$\chi(\omega, q) = \int \frac{2d^2p}{(2\pi)^2} \frac{n_{\mathbf{p}-\mathbf{q}} - n_{\mathbf{p}}}{\omega + \xi_{\mathbf{p}-\mathbf{q}} - \xi_{\mathbf{p}} + i\eta}, \quad (5)$$

where $n_{\mathbf{p}}$ is the Fermi-Dirac distribution function. In the plasmon frequency range ($\omega \gg qv_F$) the polarization operator can be approximated by $\chi(\omega, q) = mq^2 v_F^2 / (2\pi\omega^2)$, leading to the plasmon spectrum, Eq. (1).



FIG. 1: The Dyson equation for the propagator of the scalar potential (shown by the bold wavy line) in the lowest order in the electron phonon-interaction. The thin wavy line stands for the propagator evaluated in the conventional RPA approximation, $U(\omega, q) = V_q/[1 - V_q \chi(\omega, q)]$, the zigzag line represents the phonon Green function, the loop stands for the electron polarization operator $\chi(\omega, q)$.

To find the lowest-order in electron-phonon interaction correction to the dielectric function, one needs to solve the equation for the longitudinal electric field propagator, see Fig. 1. The resulting dielectric function is

$$\varepsilon(\omega, q)/\varepsilon^* = 1 - V_q \chi(\omega, q) - V_q \chi^2(\omega, q) \times \sum_\lambda \int \frac{dq_z}{2\pi} \frac{\mathcal{M}_\lambda^2(q, q_z)}{\rho[(\omega + i\eta)^2 - s_\lambda^2(q^2 + q_z^2)]}. \quad (6)$$

The plasmon spectrum $\omega = \omega_q - i\gamma_q$ is determined by a zero of the dielectric function (6). The imaginary part γ_q originates from the poles of the phonon propagator at those values of momentum q_z which satisfy the energy conservation condition, $\omega_q = s_\lambda \sqrt{q^2 + q_z^2}$. After simple calculation, with the use of the condition $|q_z| \approx \omega_q/s_\lambda \gg q$, we obtain

$$\gamma_q = \frac{mq^2 v_F^2}{8\pi\rho\omega_q^2} \sum_\lambda s_\lambda^{-1} \mathcal{M}_\lambda^2(q, \omega_q/s_\lambda). \quad (7)$$

The deformation potential interaction yields the contribution to the plasmon linewidth,

$$\gamma_q = \frac{\pi\eta_d^2 q^2 v_F^2}{4\omega_s}. \quad (8)$$

Here $\omega_s = k_F s_l$ is the characteristic phonon frequency, and

$$\eta_d^2 = \frac{mk_F \Xi^2}{2\pi^2 \rho s_l^2} \quad (9)$$

is the dimensionless coupling constant for the deformation potential interaction.

The piezoelectric coupling, contrary to the deformation potential, remains finite in the long-wavelength limit. Therefore, when present, the former often leads to much stronger effects than the latter. However, the piezoelectric contribution into the width (7) is strongly reduced due to the fact that the plasmons emit phonons almost perpendicular to the 2DEG plane, $\theta \approx qs/\omega_q \ll 1$. According to Eq. (4), the piezoelectric coupling is stronger for the transverse phonons. However, the corresponding contribution to the width Eq. (7) is still small compared to the deformation potential contribution Eq. (8), by a factor of $(s/v_F)^4 \ll 1$.

Rate of the direct (via a virtual electron-hole pair) plasmon-phonon conversion given by Eq. (7), describes the temperature-independent plasmon broadening. To analyze the temperature-dependent attenuation one has to account for the inelastic processes resulting in creation of electron-hole pairs in the final state. To do this we relate the plasmon attenuation to the optical conductivity.

III. PHONON-ASSISTED LANDAU DAMPING

The propagation of a plasmon in 2DEG is accompanied by an oscillating electric field, whose scalar potential is a plane wave in the in-plane direction \mathbf{x} and satisfies the equation $\nabla^2 \phi = 0$ outside 2DEG,

$$\phi(\mathbf{x}, z, t) = (\phi_0 e^{-i\omega t + i\mathbf{q}\mathbf{x}} + \phi_0^* e^{i\omega t - i\mathbf{q}\mathbf{x}}) e^{-q|z|}. \quad (10)$$

The energy (per unit area) of the electric field (10) is given by

$$W_e = \frac{\varepsilon^*}{8\pi} \int dz \overline{(\nabla\phi)^2} = \frac{\varepsilon^* q}{2\pi} |\phi_0|^2 = e^2 V_q^{-1} |\phi_0|^2, \quad (11)$$

where the bar denotes the in-plane average. The kinetic energy of electrons is equal to the energy of electric field (the virial theorem). The total energy of a plasmon is therefore, $W = 2W_e$. The plasmon attenuation γ_q is related to the energy dissipation rate,

$$dW/dt = -2\gamma_q W = -4\gamma_q W_e. \quad (12)$$

On the other hand dissipation is related to the real part of the longitudinal optical conductivity $\sigma'(\omega, q)$,

$$-\frac{dW}{dt} = 2q^2 |\phi_0|^2 \sigma'(\omega, q). \quad (13)$$

The right-hand side in this expression is the Joule heating. Note, that Eq. (13) can be applied to attenuation of plasma eigenmodes as well as the dissipation of the external electric field. In the latter case $q\phi_0$ should be understood as the amplitude of the electric field at the 2DEG plane. Using Eqs. (12) and (13) we can relate the plasmon attenuation to the optical conductivity at $\omega = \omega_q$,

$$\gamma_q = \frac{q^2 V_q}{2e^2} \sigma'(\omega_q, q). \quad (14)$$

Equation (14) may be viewed as the Ward identity relating $\chi(\omega, q)$ and $\sigma(\omega, q)$, *i.e.*, the polarization operators with scalar and vector vertices.

To evaluate γ_q , we find first dW/dt with the help of the perturbation theory in the interaction of electrons with phonons and with electric field ϕ_0 , see Eqs. (2) and (10). We then obtain γ_q from dW/dt with the help of Eqs. (13)–(14). We are interested in the dissipation of the high-frequency electric field, $\omega \gg qv_F$. At such frequencies, the field absorption due to an excitation of a single electron-hole pair (Landau damping) is forbidden by the energy and momentum conservation conditions. The lowest-order absorption process, therefore, includes also a creation or annihilation of a phonon, see Fig. 2. The probability of the field absorption process is given

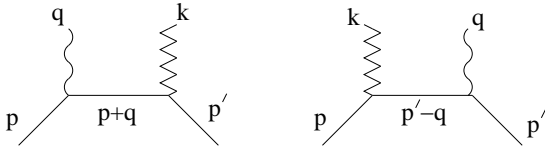


FIG. 2: Graphic representation of the transition amplitude L . Wavy lines stand for the amplitude of the electric field ϕ_0 , zigzag lines denote phonons.

by the Fermi Golden rule⁸,

$$dw_{\pm} = 2\pi |L_{\lambda}|^2 \delta(\xi_{\mathbf{p}} + \omega - \xi_{\mathbf{p}'} \mp \omega_{\lambda\mathbf{k}}) \times \delta(\mathbf{p} + \mathbf{q} - \mathbf{p}' \mp \mathbf{k}_{\parallel}) \frac{d^2 p' d^3 k}{(2\pi)^3}. \quad (15)$$

Here the matrix element

$$L_{\lambda} = \frac{e\phi_0 \varepsilon^* \mathcal{M}_{\lambda}(\mathbf{k})}{\varepsilon(\omega, k_{\parallel}) \sqrt{2\rho\omega_{\lambda\mathbf{k}}}} \times \left(\frac{1}{\xi_{\mathbf{p}} - \xi_{\mathbf{p}+\mathbf{q}} + \omega} + \frac{1}{\xi_{\mathbf{p}'} - \xi_{\mathbf{p}'-\mathbf{q}} - \omega} \right) \quad (16)$$

accounts for the intermediate state in the process, and the signs \pm correspond to the creation (annihilation) of a phonon, which accompanies the excitation of the electron-hole pair. The dielectric function in the denominator of the matrix element Eq. (16) accounts for the screening of the electron-phonon interaction by two-dimensional electrons. The presence of two terms in Eq. (16) corresponds to the two different possibilities for the virtual state depending on whether the electron interacts first with the plasmon or with the phonon, see Fig. 2. Each internal line contributes to the matrix element a propagator of the virtual state, $(E - E_v)^{-1}$, with E being the total energy of particles, and E_v the energy of the virtual state.

The resulting probability of the field absorption is given by the appropriate sum over the initial and final states of the electron-phonon system,

$$I_a = \sum_{\lambda} \int \frac{2d^2 p}{(2\pi)^2} n_p (1 - n_{p'}) [(1 + N_{\lambda\mathbf{k}}) dw_{+} + N_{\lambda\mathbf{k}} dw_{-}], \quad (17)$$

where $N_{\lambda\mathbf{k}}$ is the Bose-Einstein phonon distribution, and factor 2 takes into account the electron spin degeneracy. The probability for the field emission, I_e can be found from the detailed balance principle⁹, $I_e = I_a e^{-\omega/T}$.

The energy dissipation rate is then determined by the two probabilities,

$$-\frac{dW}{dt} = \omega(I_a - I_e) = \omega(1 - e^{-\omega/T})I_a. \quad (18)$$

In the high-frequency domain $\omega \gg qv_F$, the relevant momentum of an electron-hole pair $\mathbf{p} - \mathbf{p}'$ and that of a phonon \mathbf{k} are large compared to the plasmon momentum \mathbf{q} , which allows us to simplify the matrix element L_{λ} ,

$$L_{\lambda} = \frac{e\phi_0 \varepsilon^* \mathcal{M}_{\lambda}(\mathbf{k})}{\varepsilon(\omega, k_{\parallel}) \sqrt{2\rho\omega_{\lambda\mathbf{k}}}} \frac{(\mathbf{p} - \mathbf{p}') \cdot \mathbf{q}}{m\omega^2}. \quad (19)$$

In the last expression we also have used the momentum conservation condition Eq. (15). Combining Eqs. (13), (15) and (17)–(19), we obtain the phonon-assisted Landau damping in the form:

$$\sigma'(\omega, q) = \frac{e^2 \varepsilon^{*2} \sinh[\frac{\omega}{2T}]}{8\rho m^2 \omega^3} \sum_{\lambda} \int \frac{d^3 k}{(2\pi)^3} \frac{k_{\parallel}^2 \mathcal{M}_{\lambda}^2(\mathbf{k})}{\omega_{\lambda\mathbf{k}} |\varepsilon(\omega, k_{\parallel})|^2} \times \frac{1}{\sinh[\frac{\omega_{\lambda\mathbf{k}}}{2T}]} \left[\frac{\chi''(\omega_{\lambda\mathbf{k}} - \omega, k_{\parallel})}{\sinh[\frac{\omega - \omega_{\lambda\mathbf{k}}}{2T}]} - \frac{\chi''(\omega_{\lambda\mathbf{k}} + \omega, k_{\parallel})}{\sinh[\frac{\omega + \omega_{\lambda\mathbf{k}}}{2T}]} \right]. \quad (20)$$

Here χ'' is the structure factor of 2DEG, *i.e.*, the imaginary part of the polarization operator Eq. (5). We are interested in the optical conductivity at $\omega, T \ll E_F$, where

$E_F = k_F^2/2m$ is the Fermi energy. It allows us to use the low-frequency limit of χ'' ,

$$\chi''(\Omega, k_{\parallel}) = -\frac{m}{\pi|k_{\parallel}|v_F} \frac{\Omega}{\sqrt{1 - \left(\frac{k_{\parallel}}{2k_F}\right)^2}}.$$

This limiting form is valid across the entire particle-hole domain of excitations, except narrow regions near its ends, $|\Omega|/v_F \leq k_{\parallel} \leq 2k_F - |\Omega|/v_F$.

The electron-phonon interaction is effectively screened at a small momentum transfer between the two subsystems, which results in a strong frequency dependence of the conductivity. Indeed, since only the particle-hole domain is relevant in the integral (20), it suffices to approximate the dielectric function by its static limit, $\varepsilon(0, k_{\parallel})/\varepsilon^* = 1 + \kappa^2/k_{\parallel}^2$. The characteristic momenta in the integral of Eq. (20) are $k_{\parallel} \sim \max(\omega, T)/s$. Therefore, at $\omega, T \ll \omega_{\kappa}$ the screening of the electron-phonon interaction is strong (here we introduced the characteristic frequency $\omega_{\kappa} = \kappa s$, and κ is the inverse screening radius). We consider below the plasmon attenuation in the limits of weak and strong screening.

(i) In the limit of low frequency and temperature, $\omega, T \ll \omega_{\kappa}$, corresponding to the strong screening, a straightforward evaluation of the integral in Eq. (20) yields for the electron-phonon interaction via deformation potential,

$$\gamma_q = \frac{3\pi\eta_d^2}{7 \cdot 2^9 \omega_s^4 \omega_{\kappa}^2} \begin{cases} \omega_q^7, & \omega_q > 2\pi T, \\ A(2\pi T)^7, & \omega_q < 2\pi T, \end{cases} \quad (21)$$

where $A = 1.47$. Similarly, for the piezoelectric coupling,

$$\gamma_q = \frac{\pi\eta_p^2}{15 \cdot 2^9 \omega_s^4 \omega_{\kappa}^2} \begin{cases} \omega_q^5, & \omega_q > 2\pi T, \\ B(2\pi T)^5, & \omega_q < 2\pi T, \end{cases} \quad (22)$$

with the coefficient $B = 0.76$. Here characteristic frequencies $\omega_{\kappa} = \kappa s_l$ and $\omega_s = k_F s_l$ depend on the material parameters. The deformation potential coupling strength η_d is given in Eq. (9), and the dimensionless constant for the piezoelectric coupling is

$$\eta_p^2 = \frac{m(eh_{14})^2}{2\pi^2 \rho s_l^2 k_F} \left(\frac{63}{256} + \frac{s_l^6}{s_t^6} \frac{87}{256} \right). \quad (23)$$

Clearly, in the limit of low temperature and plasmon frequency, the piezoelectric part, Eq. (22), prevails over the deformation potential contribution Eq. (21).

(ii) We turn now to the case of a weak screening. In typical heterostructures the inverse screening radius κ is of the order of k_F , and therefore $\omega_{\kappa} \sim \omega_s$. We concentrate on relatively large frequencies or high temperatures, *i.e.*, assume that ω or T exceed ω_{κ} and ω_s , but are still small compared to the Fermi energy, $E_F = k_F^2/2m$.

The leading deformation potential contribution in Eq. (20) comes from phonon states with $k_{\parallel} \sim k_F$ and $k_z \sim \max(\omega, T)/s \gg k_F$, *i.e.*, from the phonons propagating almost normally to the 2DEG plane. In the limit

of high temperature or frequency we find

$$\gamma_q = C \frac{\eta_d^2}{\omega_s} [\omega_q^2 + (2\pi T)^2]. \quad (24)$$

Here the numerical coefficient C depends on the screening parameter $\kappa/2k_F$,

$$C = \frac{1}{3} \int_0^{\pi/2} \frac{\sin^4 \theta}{(\sin \theta + \frac{\kappa}{2k_F})^2}, \quad (25)$$

and varies from $C = \pi/12 \approx 0.26$ to $C = 0.06$ when the screening parameter increases from $\kappa/2k_F = 0$ to $\kappa/2k_F = 1$.

Unlike the interaction via deformation potential, the piezoelectric mechanism of the electron-phonon interaction is ineffective for phonons with $|k_{\parallel}| \ll k$. As the result, the piezoelectric mechanism yields a contribution to γ_q , which is smaller than the one given by Eq. (24). In particular, at low temperatures and high frequencies, $T \lesssim \omega_s \lesssim \omega$, this contribution to the plasmon line width saturates at a value

$$\gamma_q \sim \eta_p^2 \omega_s, \quad (26)$$

while in the case of high temperature, $T \gtrsim \omega_s$, we find

$$\gamma_q \sim \eta_p^2 T, \quad (27)$$

independent of the parameter ω/ω_s . Strictly speaking, the piezoelectric constants in Eqs. (26)–(27) differ from the definition Eq. (23) by the numerical coefficients in the brackets, since the angle integrals are different in each regime. However, for rough estimates, one can use Eq. (23).

IV. TWO-PAIR ABSORPTION

Another mechanism effective for the absorption of plasmons with energies ($\omega_q \ll E_F$) is associated with creation of two electron-hole excitations¹. The probability of absorption or excitation of two electron-hole pairs by an electric field Eq. (10) can be found with the help of the Golden rule by treating the field strength and the electron-electron interaction V_q perturbatively,

$$dw = 2\pi |\mathcal{L}|^2 \delta(\xi_{\mathbf{p}} + \xi_{\mathbf{k}} - \xi_{\mathbf{p}'} - \xi_{\mathbf{k}'} + \omega) \times \delta(\mathbf{p} + \mathbf{k} - \mathbf{p}' - \mathbf{k}' + \mathbf{q}) \frac{d^2 p' d^2 k'}{(2\pi)^2}. \quad (28)$$

Here \mathbf{p}, \mathbf{k} and \mathbf{p}', \mathbf{k}' are, respectively, the initial and final momenta of two electrons. The matrix element \mathcal{L} depends of the initial spin state of the two electrons. For a singlet state the transition matrix element is

$$\mathcal{L}_{0,0} = e\phi_0 \left(\frac{V_{\mathbf{k}-\mathbf{k}'} + V_{\mathbf{p}'-\mathbf{k}}}{\xi_{\mathbf{p}} - \xi_{\mathbf{p}+\mathbf{q}} + \omega} + \frac{V_{\mathbf{k}-\mathbf{k}'} + V_{\mathbf{p}-\mathbf{k}'}}{\xi_{\mathbf{p}'} - \xi_{\mathbf{p}'-\mathbf{q}} - \omega} + \frac{V_{\mathbf{p}'-\mathbf{p}} + V_{\mathbf{p}-\mathbf{k}'}}{\xi_{\mathbf{k}} - \xi_{\mathbf{k}+\mathbf{q}} + \omega} + \frac{V_{\mathbf{p}'-\mathbf{p}} + V_{\mathbf{p}'-\mathbf{k}}}{\xi_{\mathbf{k}'} - \xi_{\mathbf{k}'-\mathbf{q}} - \omega} \right), \quad (29)$$

and for a triplet state it is

$$\mathcal{L}_{1,0} = e\phi_0 \left(\frac{V_{\mathbf{k}-\mathbf{k}'} - V_{\mathbf{p}'-\mathbf{k}}}{\xi_{\mathbf{p}} - \xi_{\mathbf{p}+\mathbf{q}} + \omega} + \frac{V_{\mathbf{k}-\mathbf{k}'} - V_{\mathbf{p}-\mathbf{k}'}}{\xi_{\mathbf{p}'} - \xi_{\mathbf{p}'-\mathbf{q}} - \omega} + \frac{V_{\mathbf{p}'-\mathbf{p}} - V_{\mathbf{p}-\mathbf{k}'}}{\xi_{\mathbf{k}} - \xi_{\mathbf{k}+\mathbf{q}} + \omega} + \frac{V_{\mathbf{p}'-\mathbf{p}} - V_{\mathbf{p}'-\mathbf{k}}}{\xi_{\mathbf{k}'} - \xi_{\mathbf{k}'-\mathbf{q}} - \omega} \right). \quad (30)$$

The first subscript of the matrix element denotes the value of the total spin of two electrons, while the second subscript stands for its projection onto the z -direction. The matrix element in the triplet channel is the same for all three spin states, $\mathcal{L}_{1,0} = \mathcal{L}_{1,\pm 1}$, since the electron-electron interaction is spin-independent. The structure of the matrix elements Eqs. (29) and (30) is clear from the graphic representation shown in Fig. 3. Again, as in Fig. 2, the internal lines correspond to the virtual states whose propagators are given by $(E - E_v)^{-1}$, with E being the total energy of the particles and E_v is the energy of a virtual state. The total probability of the field absorption is given by the sum over the initial and final states according to

$$I_a = \frac{1}{4} \int \frac{d^2 p d^2 k}{(2\pi)^4} [dw_{0,0} + 3dw_{1,0}] n_p n_k (1 - n_{p'}) (1 - n_{k'}). \quad (31)$$

Here the coefficient $1/4$ prevents from double-counting of the initial and final states. The above formulas are valid

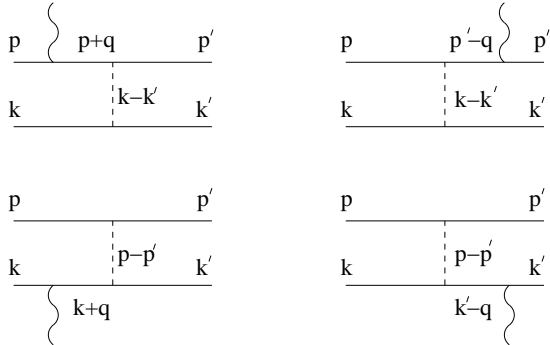


FIG. 3: Graphic representation for the two-pair absorption amplitude \mathcal{L} , see Eqs. (29)-(30). The insertion of the wavy line (external wave or plasmon) into the two-electron scattering process is possible in the shown here four different ways, corresponding to four fractions in Eqs. (29)-(30). In addition, an interchange $\mathbf{p}' \leftrightarrow \mathbf{k}'$ in the final state is possible, bringing two terms in each of the numerators in Eqs. (29)-(30). The relative signs of these terms depend on the spin state of the two electrons.

for any values of ω and q . We now make use of the fact

that $\omega \gg qv_F$ in the region of interest, and obtain

$$\begin{aligned} \mathcal{L}_{0,0} &= \frac{e\phi_0}{m\omega^2} (\mathcal{A} + \mathcal{A}_{\text{ex}}), \\ \mathcal{L}_{1,0} &= \frac{e\phi_0}{m\omega^2} (\mathcal{A} - \mathcal{A}_{\text{ex}}). \end{aligned} \quad (32)$$

Here we introduced the following notations:

$$\begin{aligned} \mathcal{A} &= \mathbf{q} \cdot [(\mathbf{Q} + \mathbf{q})V_{\mathbf{Q}+\mathbf{q}} - \mathbf{Q}V_{\mathbf{Q}}] \\ \mathcal{A}_{\text{ex}} &= \mathbf{q} \cdot [(\mathbf{p}' - \mathbf{k})V_{\mathbf{p}'-\mathbf{k}} + (\mathbf{k}' - \mathbf{p})V_{\mathbf{p}-\mathbf{k}'}], \end{aligned} \quad (33)$$

and accounted for the momentum conservation evident from Eq. (28). The momentum transferred in a collision is denoted by $\mathbf{Q} = \mathbf{p} - \mathbf{p}'$. The term \mathcal{A}_{ex} is obtained from \mathcal{A} by interchanging the momenta $\mathbf{p}' \leftrightarrow \mathbf{k}'$, and originates from the indistinguishability of colliding particles.

The transition rates given by Eq. (28) with the matrix elements Eq. (32) determine the total probability of absorption Eq. (31). As usual, the total probability of emission I_e is related to the probability of absorption by the detailed balance principle, $I_e = I_a e^{-\omega/T}$. The energy dissipation rate dW/dt can be expressed in terms of the probability I_a according to Eq. (18). The optical conductivity is then obtained from its relation to dW/dt , represented by Eq. (13),

$$\begin{aligned} \sigma'(\omega, q) &= \frac{e^2(1 - e^{-\omega/T})}{m^2\omega^3q^2} \int \frac{d^2 p d^2 k d^2 p' d^2 k'}{(2\pi)^5} \\ &\times \mathcal{A} (\mathcal{A} - \mathcal{A}_{\text{ex}}/2) \delta(\xi_{\mathbf{p}} + \xi_{\mathbf{k}} - \xi_{\mathbf{p}'} - \xi_{\mathbf{k}'} + \omega) \\ &\times n_p n_k (1 - n_{p'}) (1 - n_{k'}) \delta(\mathbf{p} + \mathbf{k} - \mathbf{p}' - \mathbf{k}' + \mathbf{q}). \end{aligned} \quad (34)$$

The optical conductivity Eq. (34) vanishes as $\sigma'(\omega, q) \propto q^2$ in the long-wavelength limit $q \rightarrow 0$. This is clear from the small- q properties of the amplitudes \mathcal{A} and \mathcal{A}_{ex} . Indeed, the relation $\mathcal{A} \propto q^2$ at $q \rightarrow 0$ follows directly from the first line of Eq. (33), and the relation $\mathcal{A}_{\text{ex}} \propto q^2$ can be obtained from the second line of Eq. (33) and the momentum conservation condition. The absence of absorption in the long-wavelength limit, $\sigma'(\omega, q = 0) = 0$, is a manifestation of a more general principle¹⁰: a translationally invariant electron liquid does not absorb energy from an applied uniform ac field. From a technical standpoint, the zero value of $\sigma'(\omega, q = 0)$ comes as the result of a cancellation of the four matrix elements, Fig. 3, of which any element is not small by the external wave vector q . Recently, Gornyi and Mirlin¹¹ demonstrated a

similar cancellation in the diagrammatic calculation of the homogeneous conductivity, while Pustilnik et. al. encountered q^2 -behavior in the calculation of the far tails of the density-density correlation function in the case of spinless one-dimensional fermions¹². This cancellation was overlooked by Reizer and Vinokur in their calculation of the attenuation of two-dimensional plasmons¹³. It led to a result large by a factor k_F^2/q^2 , in contradiction with the above mentioned general principle.

The contribution of the exchange term \mathcal{A}_{ex} to the conductivity Eq. (34) can be estimated from Eq. (33). This contribution involves large transferred momenta $|\mathbf{p}' - \mathbf{k}| \sim k_F$, whereas the small-momentum domain of $\mathbf{Q} = \mathbf{p} - \mathbf{p}'$ is important for the contribution of \mathcal{A} . Typical values of Q in Eq. (34) can be estimated from the conservation of energy, $Q \sim \max(\omega, T)/v_F$. From Eq. (33) we then obtain $\mathcal{A}_{\text{ex}}/\mathcal{A} \sim V_Q/V_{k_F}$. The amplitude \mathcal{A}_{ex} can thus be neglected in Eq. (34), if the interaction potential is long-ranged, $V_Q \ll V_{k_F}$. This condition is met for Coulomb interaction at $\omega, T \ll E_F$. In this case the scattering amplitudes are the same for singlet and triplet states.

Neglecting the exchange contribution one can conveniently represent the optical conductivity in terms of the structure factors for free electrons,

$$\sigma'(\omega, q) = \frac{e^2 \sinh[\frac{\omega}{2T}]}{2\pi m^2 \omega^3 q^2} \int \frac{d^2 Q}{(2\pi)^2} [\mathbf{q} \cdot (\mathbf{Q} + \mathbf{q}) V_{\mathbf{Q}+\mathbf{q}} - \mathbf{q} \cdot \mathbf{Q} V_{\mathbf{Q}}]^2 \int_{-\infty}^{\infty} d\Omega \frac{\chi''(\Omega, \mathbf{Q}) \chi''(\Omega + \omega, \mathbf{Q} + \mathbf{q})}{\sinh[\frac{\Omega}{2T}] \sinh[\frac{\Omega + \omega}{2T}]}. \quad (35)$$

The formula (35) describes energy dissipation due to the decay into two electron-hole pairs with energies and momenta $\Omega + \omega, \mathbf{Q} + \mathbf{q}$ and $-\Omega, -\mathbf{Q}$, respectively. The densities of the electron-hole pairs are determined by the structure factors χ'' .

In the case of Coulomb interaction, $[\mathbf{q} \cdot (\mathbf{Q} + \mathbf{q}) V_{\mathbf{Q}+\mathbf{q}} - \mathbf{q} \cdot \mathbf{Q} V_{\mathbf{Q}}]^2 \propto q^4/Q^2$. The momentum integral in Eq. (35) is, therefore, singular at small values of Q . If the smallest value of $Q = \omega/2v_F$, allowed by the energy conservation condition, becomes smaller than the inverse screening radius κ , then the screening of Coulomb interaction must be accounted for. This is achieved by the replacement of the interaction potential V_Q in Eq. (35) by its screened value. As in the case of the phonon-assisted conductivity, it is sufficient here to account for the dielectric function by using its static limit, $V_Q \rightarrow \varepsilon^* V_Q/\varepsilon(0, Q)$. An emphasis on the small- Q domain comes also from the structure of the density of states of the electron-hole pairs. Indeed, integration over frequencies Ω in Eq. (35) results in an additional factor $\propto Q^{-2}$. Therefore, if the calculation is to be performed with the logarithmic in κ_F/ω accuracy, we can neglect the difference between $V_{Q+\mathbf{q}}$ and V_Q , and

simplify Eq. (35) to

$$\sigma'(\omega, q) = \frac{e^2 q^2 \sinh[\frac{\omega}{2T}]}{\pi m^2 \omega^3} \int_0^{\infty} \frac{Q dQ}{2\pi} \int_{-\infty}^{\infty} d\Omega \times \frac{V_Q^2 \varepsilon^{*2}}{\varepsilon^2(0, Q)} \frac{\chi''(\Omega_+, Q) \chi''(\Omega_-, Q)}{\cosh[\frac{\Omega}{2T}] - \cosh[\frac{\omega}{2T}]}, \quad (36)$$

where $\Omega_{\pm} = \Omega \pm \omega/2$. In the long-wavelength limit, $Q \ll k_F$, the structure factor has the form

$$\chi''(\Omega, Q) = -\frac{m\Omega}{\pi \sqrt{Q^2 v_F^2 - \Omega^2}} \theta(Q v_F - |\Omega|). \quad (37)$$

To evaluate the conductivity Eq. (36), it is technically more convenient to change the order of integrations and evaluate first the integral over the momentum. With the logarithmic accuracy, the integral is cut at the upper limit $Q \sim \kappa$, leading to the following integral over frequency,

$$\sigma'(\omega, q) = \frac{e^2 q^2 \sinh[\frac{\omega}{2T}]}{\pi^2 k_F^2 \omega^3} \times \int_0^{\infty} d\Omega \frac{(\frac{\omega}{2})^2 - \Omega^2}{\cosh[\frac{\omega}{2T}] - \cosh[\frac{\Omega}{T}]} \ln \left[\frac{\kappa v_F}{\sqrt{\Omega \omega}} \right]. \quad (38)$$

Utilizing the fact that the logarithm is a slow function of its argument, one can evaluate the integral in Eq. (38) with the logarithm assigned its value at the characteristic frequency $\Delta = \max(\omega, 2\pi T)$. The two-pair contribution to the optical conductivity takes the form

$$\sigma'(\omega, q) = \frac{e^2 q^2}{12\pi^2 k_F^2 \omega^2} [\omega^2 + (2\pi T)^2] \ln \left[\frac{\kappa v_F}{\sqrt{\omega \Delta}} \right]. \quad (39)$$

Finally, the plasmon attenuation is found from its relation Eq. (14) to the optical conductivity,

$$\gamma_q = \frac{q^2}{24\pi k_F^2 E_F} [\omega_q^2 + (2\pi T)^2] \ln \left[\frac{\kappa v_F}{\sqrt{\omega_q \Delta_q}} \right], \quad (40)$$

where $\Delta_q = \max(\omega_q, 2\pi T)$. The expression (40) weakly depends on the strength of the electron-electron interaction. This is due to the fact that the principal contribution to the conductivity comes, with logarithmic accuracy, from the momentum range $Q < \kappa$, where interaction is screened. Our calculation is, therefore, correct as long as the Fermi momentum exceeds the inverse screening radius, $k_F \gg \kappa$. In a realistic 2DEG, however, the two quantities are of the same order of magnitude. In this general case it is no longer a good approximation to disregard the scattering with large momenta $Q \sim k_F$ and to neglect the exchange effects represented by the amplitude \mathcal{A}_{ex} in Eq. (34). One should expect the numerical coefficient in Eqs. (39)–(40) to change and become interaction-dependent for $\kappa \gtrsim k_F$.

V. NUMERICAL ESTIMATES FOR A GaAs HETEROSTRUCTURE

In this Section we compare the effectiveness of different mechanisms contributing to the attenuation of plasmons. We concentrate on the case of low temperature, and consider attenuation γ_q as a function of the plasmon energy $\hbar\omega_q$.

In the important case of a GaAs heterostructure, the material parameters are^{3,6,14}: deformation potential coupling constant $\Xi = 2.2 \times 10^{-18}$ J, piezoelectric constant $h_{14} = 1.38 \times 10^9$ V m⁻¹, longitudinal sound velocity $s_l = 5.2 \times 10^3$ m s⁻¹, transverse sound velocity $s_t = 3.0 \times 10^3$ m s⁻¹, crystal density $\rho = 5.3 \times 10^3$ kg m⁻³, and the dielectric constant $\varepsilon^* = 12.8$. For estimates, we take a typical Fermi momentum, $k_F \approx 1 \times 10^8$ m⁻¹, which corresponds to the Fermi energy $E_F \approx 5.6$ meV.

Using Eqs. (9) and (23) we find the dimensionless electron-phonon coupling strengths: $\eta_d = 0.03$ for the deformation potential, and $\eta_p = 0.09$ for the piezoelectric coupling. The characteristic frequencies ω_s and ω_κ , introduced after Eqs. (8) and (22) respectively, are of the same order, $\hbar\omega_\kappa \approx 0.7$ meV, and $\hbar\omega_s \approx 0.3$ meV.

Comparison of Eqs. (8), (21), (22), and (40) with each other shows that the plasmon-phonon conversion mechanism yielding $\gamma_q \propto \omega_q^4$, see Eq. (8), dominates the attenuation only at very low plasmon energies, $\hbar\omega_q \lesssim 0.02$ meV. At higher energies, the phonon-assisted Landau damping via piezoelectric coupling prevails, and $\gamma_q \propto \omega_q^5$ as long as $\hbar\omega_q \lesssim 2\omega_s \approx 0.7$ meV. At higher energies, the piezoelectric contribution saturates, see Eq. (26), while the contribution coming from the deformation potential interaction, Eq. (24), monotonically increases, $\gamma_q \propto \omega_q^2$. It becomes the dominant one at $\hbar\omega_q \gtrsim 1$ meV, and exceeds the two-pair mechanism, Eq. (40), by a factor $\sim (E_F/\omega_q)^4$ in the entire range $\hbar\omega_q \lesssim E_F$. We are not considering higher plasmon energies, where the conventional Landau damping significantly contributes to the plasmon line width.

VI. CONCLUSIONS

We presented a theory for the real part of the optical conductivity $\sigma'(\omega, q)$ of a ballistic 2DEG at finite wave-vectors and utilized it for calculation of a plasmon width. Collisionless energy dissipation (Landau damping) in a degenerate plasma is exponentially small $\sim \exp[-m\omega_q^2/2q^2T]$ in the low-temperature and long-wavelength limit. That prompted us to consider a number of mechanisms which would be sub-leading, should conservation laws allow for the Landau damping. These mechanisms are the plasmon-phonon conversion, see Section II, phonon-assisted creation of an electron-hole pair, see Section III, and two-pair absorption, see Section IV. In the domain of low plasmon energies and low temperatures, $\hbar\omega_q, T \lesssim E_F$, all the found contributions have

power-law (in ω_q and T) asymptotes, see Eqs. (8), (21), (22), (26), (27), and (40). The smallest exponent belongs to the conversion mechanism, which therefore dominates the plasmon line width at the lowest temperatures. (We do not discuss here a competing contribution from the impurity scattering.) The relative importance of the other considered mechanisms at higher temperatures depends on the material parameters. In the important case of a GaAs heterostructure, apparently the two-pair mechanism does not become the leading one, see Section V. This mechanism, however, results in a ‘‘universal’’ contribution, see Eq. (40), which is only weakly (logarithmically) dependent on the parameters of the host material.

VII. ACKNOWLEDGEMENTS

We acknowledge fruitful discussions with A. Andreev, E. Demler, B. Halperin, A. Kamenev, D. Maslov, P. Platzman, M. Pustilnik and V. Vinokur. E.M. is grateful to the University of Minnesota for hospitality, and M.R. thanks Aspen Center for Physics. The research at Harvard University was supported by NSF grant DMR02-33773, and at the University of Minnesota by NSF grants DMR02-37296 and EIA02-10736. E.M. also acknowledges the support from the Russian Foundation for Basic Research, project # 04-02-17087.

APPENDIX A: PLASMON-PHONON CONVERSION RATE IN THE GOLDEN RULE APPROXIMATION

The plasmon-phonon conversion rate, Eq. (7), can also be derived from the Golden rule formalism similar to the phonon-assisted Landau damping and the two-pair attenuation rate. The probability of electric field absorption accompanied by the phonon emission, Fig. 4, is given by the expression,

$$dw_{\lambda\mathbf{k}} = 2\pi e^2 |\phi_0|^2 \chi^2(\omega, q) \frac{\mathcal{M}_{\lambda}^2(\mathbf{k})}{2\rho\omega_{\lambda\mathbf{k}}} \delta(\omega - \omega_{\lambda\mathbf{k}}) \times \delta(\mathbf{q} - \mathbf{k}_{\parallel}) \frac{d^3k}{2\pi}. \quad (\text{A1})$$

After summation over phonon states, the total probability of the field absorption becomes



FIG. 4: Transition amplitude for the direct conversion of the electric field (wavy line) to a phonon (zigzag line). The loop stands for the electron polarization operator $\chi(\omega, q)$.

ity of the field absorption becomes

$$I_a = \sum_{\lambda} \int (1 + N_{\lambda\mathbf{k}}) dw_{\lambda\mathbf{k}}. \quad (\text{A2})$$

The total probability of the field emission (accompanied by the phonon annihilation), I_e , is obtained from Eq. (A2) by changing $1 + N_{\lambda k} \rightarrow N_{\lambda k}$. As always, the two probabilities are related by the detailed balance condition, $I_e = I_a e^{-\omega/T}$. The corresponding contribution to the optical conductivity is found from Eqs. (18) and (13),

$$\sigma'(\omega, q) = \frac{e^2 \chi^2(\omega, q)}{2\rho q^2} \sum_{\lambda} s_{\lambda}^{-1} \mathcal{M}_{\lambda}^2(q, \omega/s_{\lambda}). \quad (\text{A3})$$

Finally, the plasmon attenuation is determined by Eq. (14),

$$\gamma_q = \frac{\chi(\omega_q, q)}{4\rho} \sum_{\lambda} s_{\lambda}^{-1} \mathcal{M}_{\lambda}^2(q, \omega_q/s_{\lambda}), \quad (\text{A4})$$

which is equivalent to Eq. (7).

-
- ¹ D.F. DuBois and M.G. Kivelson, Phys. Rev. **186**, 409 (1969).
² P.J. Price, Surf. Sci. **113**, 119 (1982); **143**, 145 (1984).
³ E.E. Mendez, P.J. Price and M. Heiblum, Appl. Phys. Lett. **45**, 294 (1984).
⁴ W. Walukiewicz, H.E. Ruda, J. Lagowski, and H. C. Gatos, Phys. Rev. B **29**, 4818 (1984).
⁵ G.D. Mahan, in *Polarons in Ionic Crystals and Polar Semiconductors*, edited by J.T. Devreese (North-Holland/American Elsevier, Amsterdam, 1972), p. 553.
⁶ J.D. Zook, Phys. Rev. **136**, A869 (1964).
⁷ H. Bruis, K. Flensberg and H. Smith, Phys. Rev. **48**, 11144 (1993).
⁸ L.D. Landau and E.M. Lifshitz, *Quantum Mechanics:*

- Non-relativistic Theory* (Addison-Wesley, Reading, Mass., 1965).
⁹ L.D. Landau and E.M. Lifshitz, *Electrodynamics of Continuous Media* (Pergamon, Oxford, 1984).
¹⁰ D. Pines and P. Nozieres, *The Theory of Quantum Liquids* (Benjamin, New York, 1966).
¹¹ I.V. Gornyi and A.D. Mirlin, Phys. Rev. B **69**, 045313 (2004).
¹² M. Pustilnik, E.G. Mishchenko, L.I. Glazman, and A.V. Andreev, Phys. Rev. Lett. **91**, 126805 (2003).
¹³ M.Yu. Reizer and V.M. Vinokur, Phys. Rev. B **62**, R16306 (2000).
¹⁴ J.S. Blakemore, J. Appl. Phys. **53**, R123 (1982).